Civil Engineering Infrastructures Journal xx,xx

DOI: 10.22059/ceij.2025.391496.2266

Analysis of Fiber Bragg Grating Sensor for CFRP Beam Crack Growth

Anitha Kumari S.D[1], Malathi S[2], Supriya M[3] and Bheem Pratap[4*]

[1]Professor, Department of Civil Engineering, M S Ramaiah University of Applied Sciences, 560058, India, Email: anithakumari.ce.et@msruas.ac.in

[2]Professor, Department of Electronics and Communication Engineering, Graphic Era (Deemed to be University), Dehradun, Uttarakhand-248002, India, Email: s.malathi.ece@geu.ac.in

[3]M. Tech. Scholar, Department of Civil Engineering, M S Ramaiah University of Applied Sciences, 560058, India, Email: supriyamanvikar1103@gmail.com

[4]Assistant Professor, Department of Civil Engineering, Graphic Era (Deemed to be University), Dehradun, Uttarakhand-248002, India. Email: bheempratapbind009@gmail.com

Received: 07/03/2025

Revised: 26/05/2025

Accepted: 02/08/2025

Abstract

This study investigates the use of a Fiber Bragg Grating (FBG) sensor to measure strain in Carbon Fiber Reinforced Polymer (CFRP)-strengthened concrete beams. Finite element analysis in Abaqus™ simulates three-point bending tests to compare the behavior of Reinforced Cement Concrete (RCC) and CFRP beams under mechanical and thermal loading.

The objective is to evaluate deflection progression until crack initiation. Simulations reveal that CFRP beams exhibit an 86% reduction in stress and strain fluctuations compared to conventional RCC beams. FBG sensor data from numerical models show strain sensitivities of 1.81 μm/μƐ for RCC and 1.21 μm/μƐ for CFRP beams, confirming the sensor's effectiveness in monitoring structural response.Thermal strain sensitivity of the simulated sensors is 1.72 nm/°C for RCC beams and 1.19 nm/°C for CFRP beams. CFRP-strengthened beam showed a significantly reduced displacement of 0.0727 mm. The proposed FBG strain sensor can be used to measure micro strains with small amplitudes in harsh environments.

Keywords: Bragg Grating, Fiber sensor, Optical sensor and Structural health Monitoring.

Nomenclature

E	Young's Modulus of the material (kN/m^2)
V	Poisson's ratio
I	Moment of inertia
E	Strain
B	Breadth of the beam
D	Depth of the beam
L	Length of beam
W	Load
$ʎ_b$	Bragg wavelength
Λ	Pitch of grating
N_{eff}	Refractive index
$P_{i,j}$	Pockels's coefficients of the strain optic sensor

Abbreviations and acronyms

SHM	Structural Health Monitoring
RCC	Reinforced Cement Concrete
CFRP	Carbon Fiber Reinforced Polymer
FEM	Finite Element Method
FOS	Fiber Optic Sensor

FBG	Fiber Bragg Grating
MZI	Mach Zehnder Interferometer
BODTA	Brillouin Optical Time Domain

Introduction

Structural Health Monitoring (SHM) is critical for determining a structure's safety and integrity in a cost-effective way. SHM integrates sensing intelligence into the process of identifying defects and also enables the recording, analysis, localization, and prediction of structure loading and damaging conditions in such a way that non-destructive testing becomes an integral part of the structure(Liu et al., 2025). Conventionally single point sensors are deployed to measure the distress in a structure(Deng et al., 2022; Sourisseau et al., 2022; Ikeda et al., 2024). However, the challenges involved in those sensors, especially the positioning of the sensors and the exposure to various harsh environments and reactions have posed difficulty in the monitoring of the performance of the structure throughout its length(Jovarauskaite et al., 2025). In this context, the application of fibre optic sensors over conventional strain gauges and accelerometers have gained significance(Sellami et al., 2025). A recent study reported by (Sakiyama et al., 2021) gives a concise review of the health monitoring of concrete structures using fibre optic based sensors. Hence this research focuses on the applications of fibre optical sensors in structural health monitoring(Tiwari et al., 2025). Generally, structural damage occurs as a result of ageing, poor construction management and lack of quality control, continuous harsh environmental exposure or in-service loading(Sellami et al., 2025). These factors can lead to structural defects on both the internal and external surfaces such as cracking, shrinkage and corrosion(Anastasopoulos et al., 2022; Benazzo et al., 2022; Harle, 2024). Cracking is a sign of concrete ageing and pathological changes, which are extremely detrimental to concrete structures (Bersan et al., 2018).

Cracks are generally considered as the most common manifestation of structural damage (Alam and Al Riyami, 2018). The propagation of internal or external cracks may result in severe damage to the structure as time progresses (Sellami et al., 2025). Further research by Bao et al. (2013), Chen et al. (2015), and Sakiyama et al. (2021) has explored strain transfer mechanisms in Brillouin sensors, particularly near strain singularities(Bao et al., 2013; Chen et al., 2015; Sakiyama et al., 2021). Theoretical and experimental results confirm that strain discontinuities reliably indicate crack locations (Srivastava et al., 2020).

Tan et al. demonstrated that quasi-distributed interrogation of FBG arrays using stepped IOFDR systems can mask strain discontinuity effects through spatial averaging (Tan et al., 2021). Fernando et al. (2017) employed FBG sensors to monitor temperature and strain development in concrete beams during the critical 28-day curing period and subsequent structural loading(Fernando et al., 2017). Their experimental setup embedded FBG sensors and thermocouples during casting, followed by combined mechanical (three-point bending) and thermal (200°C) loading post-curing. These physical tests were complemented by comprehensive FEA modeling in ABAQUS for both structural and thermal behaviors. Kaklauskas et al. (2019) developed specialized experimental configurations to obtain high-resolution reinforcement strain data using FBG sensors, comparing results with optical strain gauges(Kaklauskas et al., 2019). Subsequent numerical analysis employed stress transfer methods to calculate strain distribution along reinforced concrete elements (Deng et al., 2020; Lima et al., 2022; Zhang et al., 2024). The exceptional properties of FRP materials have led to their increasing adoption in structural rehabilitation in retrofit applications. Research embedded FBG sensors at the concrete-CFRP interface to study debonding mechanisms in strengthened structures.

Liu et al. (2017) developed an innovative curvature measurement system combining a Mach-Zehnder Interferometer (MZI) with Photonic Crystal Fiber (PCF) technology(Liu et al., 2017). Comparative analysis showed FBG sensors provided more precise but less sensitive measurements than the MZI system. The compact FBG design proved particularly effective for structural characterization due to its small footprint (Deng et al., 2021). Mao et al. investigated BOTDA and FBG, a combined approach based on the mechanical principles of concrete expansion cracking (Mao et al., 2016). Before cracking, it was observed that there was a similar variation in fibre strain from BOTDA and Bragg wavelength shift in FBG(Ye et al., 2022). This implies that the entire corrosion process is monitored solely by FBG, implying that monitoring costs will be relatively low, given the high cost of BOTDA equipment. As a result, he concluded that prior to implementing this novel sensor in a specific project, a calibration experiment should be conducted. The use of a packaged fiber-based in-line MZI for curvature sensing and crack monitoring in lightweight foamed concrete structural applications (LWFCS). They have developed polypropylene packaging for the beam's actual sensing environment, which protects the MZI sensor from harsh conditions. MZI sensors were used to define the ideal curvature sensitivity in terms of packaging thickness at various operating wavelengths (Deng et al., 2021). A FBG sensor to investigate Crack Mouth Opening Displacement (CMOD)

in concrete fractures. The FBG-based sensor is used to estimate the CMOD in plain concrete beams subjected to three-point bending tests using a digitally controlled Universal Testing Machine (UTM). The results of the FBG are compared to those of the Linear Variable Differential Transformer (LVDT). Saleem et al. reported experimental studies on the failure mechanisms on RC beams strengthened with CFRP reinforcements (Saleem et al., 2019). The crack pattern monitored in this study showed the propagation of cracks along the beam and the necessity to monitor the crack growth continuously across the beam(Gomes et al., 2025). Sevillano et al. conducted research on the development of monitoring technologies capable of being used in conjunction with modern CFRP reinforcement techniques (Sevillano et al., 2016). FBGs to monitor the damage evolution and successfully predict the appearance of debonding at the FRP-concrete interface(Wang et al., 2025). However, the results obtained from direct impedance analysis of the data collected by the FBGs sensors, that can be used to estimate the location of the multiple decoding sources, are significantly more accurate(Manterola et al., 2020). Shishkin et al. investigated strain and temperature parameters using FBGs sensors embedded in CFRP (Shishkin et al., 2016). This technique is based on the two-fiber technique, in which two FBGs are nested together and function as a single sensing element embedded in different fibres with varying strain and temperature sensitivities(Wang et al., 2025). FOSs, specifically distributed strain sensors, represent a powerful new sensing technology that is particularly well suited for monitoring strain in concrete structures(Liu et al., 2022). They are compact yet robust, capable of measuring properties within the interior of a structure without disturbing the concrete(Holmes et al., 2020). The fibre optic sensors are a promising sensing technology for civil (Structural Health Monitoring) SHM systems(Mandal and Sidhishwari, 2025). A system by integrating the technologies of (Brillouin Optical Time Domain) BOFDA and FBG to identify the cracks formed internally or externally in reinforced concrete structural elements and determine the width of the surface cracks. The results indicate that the BOFDA is very effective in detecting the location of internal cracks by placing BOFDA at different locations. The propagation of the cracks and its widening to surface cracks were studied using FBG sensors(Ye et al., 2022).

Rousan et al. (2024) conducted a nonlinear finite element analysis to assess the cyclic behavior of circular concrete-filled steel tube columns affected by alkali-silica reaction and strengthened with varying layers of CFRP. Their findings indicated that CFRP wrapping at the column ends effectively mitigated local buckling and enhanced strength, drift capacity, and energy absorption. Specifically, columns with 6 to 8 CFRP layers restored performance levels

corresponding to ASR damage levels 1 to 3, respectively(Rousan et al., 2024). Song et al. (2023) experimentally investigated recycled concrete columns with varying degrees of seismic damage, subsequently strengthened with CFRP. The study revealed that CFRP strengthening significantly improved energy dissipation, particularly in columns with moderate seismic damage. For instance, the cumulative energy dissipation increased by 32.5% in moderately damaged specimens compared to unstrengthened counterparts(Song et al., 2023).

From the literature survey, we observe optical sensors such as distributed strain sensors; represent a powerful novel sensing technology and are well suited to monitoring strain in concrete structures(Han et al., 2025; Soman et al., 2025; Zhang et al., 2025). Fiber optic sensors being compact in size, light weight and high precision are ideally suited for monitoring the structural health of reinforced concrete(Alhussein et al., 2025; Liu et al., 2025). Literature review on various types optical fiber sensors in structural health monitoring have been carried out and the research gaps were found that the crack detection using FBG on CFRP structure was not conducted. The proposed research work provides outline for combining Optical and Structural parameters towards the interdisciplinary research involving modelling and simulation. This will pave way for Opto-mechanical coupling analysis towards Structural Health Monitoring (SHM) early warning in case of natural calamities such as landslides. The present study focuses on prediction of cracks formation in CFRP concrete beam using Fiber Bragg Grating sensor. Therefore, to get most precise sensitivity of FBG sensor it is necessary to numerically analyze the concrete beam. To detect the crack development in carbon fiber reinforced polymer beam subjected to three pointing bending test using Fiber Bragg Grating sensor. The objective of this study is to explore different fiber optic sensors for crack detection, numerically model and validate a reinforced concrete beam under a three-point bending test, develop an FBG model for predicting the deflection of a CFRP beam, and assess the sensitivity of FBG for crack detection.

Methodology for the selection of fiber optic sensor

Different fibre optic sensors are in use to detect physical, mechanical or chemical parameters in various structures like dams, bridges and sewage pipelines. Among the different sensors in use, Mach-Zehnder Interferometer (MZI), Brillouin Optical Time Domain Analysis (BOTDA) and Fiber Bragg Grating (FBG) are the three major fibre optic sensors used to detect cracks in structures. Based on the theoretical formulations of the phase shift of MZI, Brillouin frequency shift of BOTDA and wavelength shift of FBG, the mathematical equations are modelled and simulated. A sensitivity analyses is done to arrive at the best suitable optical sensor for crack

detection. According to the results, BODTA has a higher sensitivity than MZI and FBG sensors. A detailed comparison indicated that the time required for measurement when FBG is used is much lesser than MZI and BODTA sensors. Also FBG sensors are more compact in size than the other two sensors, allowing for simple and hassle-free installation. Another significant advantage of FBG over other sensors is its wide temperature ranges which makes it suitable for various environmental conditions. Thus, a comprehensive consideration of all parameters lead to the conclusion that FBG is the best FOS for structural health monitoring. Hence in this study, FBG is selected as the sensing technology to measure the crack initiation and propagation in CFRP beams subjected to bending test.

The advantages of Fiber Bragg Grating based sensor over other technologies are FBG sensors are immune to Electro Magnetic Interference (EMI), FBG sensors are compact in size and can be embedded while constructing the structure and continuous monitoring is feasible and these optical sensors are capable of simultaneous measurement of accurate strain, temperature and displacement with required configuration in real time(Ye et al., 2014; K et al., 2024; Alhussein et al., 2025). The disadvantages of Fiber Bragg Grating based sensor over other technologies are fabrication of FBG requires specialized writing set up and can be overcome by customized procurement from vendors; FBG sensor interrogators are expensive and needs protection against theft at installation site and processing of the data generated by the sensors needs advanced techniques such as Machine learning algorithm to get an inference. Few researchers including our team is working towards calibration aspect(Ye et al., 2014; K et al., 2024; Alhussein et al., 2025).

Practical benefit

FBG sensors are highly sensitive to strain and deformation, which is essential for accurately tracking crack initiation and growth in CFRP beams. They can be embedded or surface-mounted without affecting the structural performance. By continuously tracking crack growth, FBG sensors help prevent catastrophic failures in CFRP structures, enhancing safety in civil engineering. FBG sensors eliminate the need for frequent manual inspections by providing automated data collection (Alhussein et al. 2025).

Economic benefit

Early detection minimizes the need for emergency repairs, thereby reducing maintenance costs and avoiding potentially costly downtime in critical infrastructure. This reduces the need for

multiple standalone sensors and wiring systems, thereby lowering installation and instrumentation costs while maintaining high-resolution monitoring. This automation translates into reduced labour costs, less downtime, and more efficient use of resources, especially for remote or hard-to-access structures (Ye et al. 2014).

Fiber optic sensors for crack detection

The fiber optic sensors are also called as optical fiber sensors. These sensors use optical fiber as sensing element. FOSs are supreme for sensitive conditions like high vibration, extreme heat, wet and unstable environments. The wavelength shift can be calculated using device, optical frequency domain reflectometry. The time-delay of the FOSs can be decided using a device OTDR.

FBGs are made by laterally exposing the core of a single-mode fiber to a periodic pattern of intense laser light. The Bragg wavelength of FBG sensor changes due to induced change in pitch length (Λ) of the grating and the perturbation of the effective core refractive index (n_{eff}) as shown in Eq. (1).

$$\lambda_B = 2n_{eff}\Lambda \quad \text{.....(1)}$$

The Bragg wavelength shift is given by equation 2:

$$\Delta\lambda_B = \lambda_B \left[1 - \left(\frac{n_{eff}2}{2}\right)[\rho_{12} - \nu(\rho_{11} + \rho_{12})]\right] * \varepsilon_Z \quad \text{.....(2)}$$

Where, $\Delta\lambda_B$=shift in Bragg wavelength

λ_B = initial wavelength

ε_z = applied strain

n_{eff} = effective refractive index of the fiber

ν = poison's ratio

$P_{i,j}$ = Pockels's coefficients of the strain optic sensor

Modelling of FBG sensor for prediction of crack

A FBG is a passive optical component in an optical fiber and is one of the most widely used optical fiber sensors. FBGs are formed by periodic variation of refractive index imprinted directly into the core of glass optical fiber by exposing to ultraviolent radiation. The specific characteristic of FBG sensor for sensing applications in periodicity causes them to act as wavelength sensitive reflectors. It is a spectrometric based fiber optic sensor, where change in wavelength of the propagating light is considered for measuring various physical parameters. In addition, the characteristic of FBG reflects a specific wavelength which shifts slightly depending on the strain applied are ideal for mechanical sensing. By considering a typical value of effective refractive index n_{eff} as 1.448 and (Λ) 524.58 nm (Pitch of the grating), we arrive at Bragg wavelength λ_B as 1519 nm. The shift in Bragg wavelength using above equation analyzed for the strains obtained from the numerical analysis of concrete beam and CFRP beam.

Carbon Fiber Reinforced Polymer (CFRP)

The method of strengthening of existing RCC structures using composites has achieved great interest over several years. Fiber Reinforced Polymers (FRP) composites have great attention as material choice for variety of applications in repair and strengthening projects(Bernasconi et al., 2022). IS 456 (2000) has been used for the design and loading of concrete beams (IS 456, 2000). The FRP composites have several advantages when compared to traditional construction materials such as steel, wood and concrete. FRPs offer excellent corrosion resistance as well as the advantages of high stiffness- to-weight and strength-to-weight ratio when compared to conventional construction materials. The apparent high cost of FRP compared to conventional materials has been a major obstacle. The deflection of RC beams strengthened with Carbon Fiber-Reinforced Polymers (CFRP) is analyzed by 3-point bending test.

Numerical modelling of CFRP beam

The CFRP beam of dimension 100 mm x 250 mm x 1400 mm is subjected to three-point bending arrangement as shown in Figure 1. The RC beam is strengthened by considering 0.9% of CFRP. The materials used for modelling CFRP beam shown in Table 1.

Table 1 Material properties of CFRP beam

Material	Modulus of elasticity (kN/m^2)	Poisson's ratio

CFRP Concrete	$2.28x10^5$	0.21
Steel	$2x10^5$	0.33

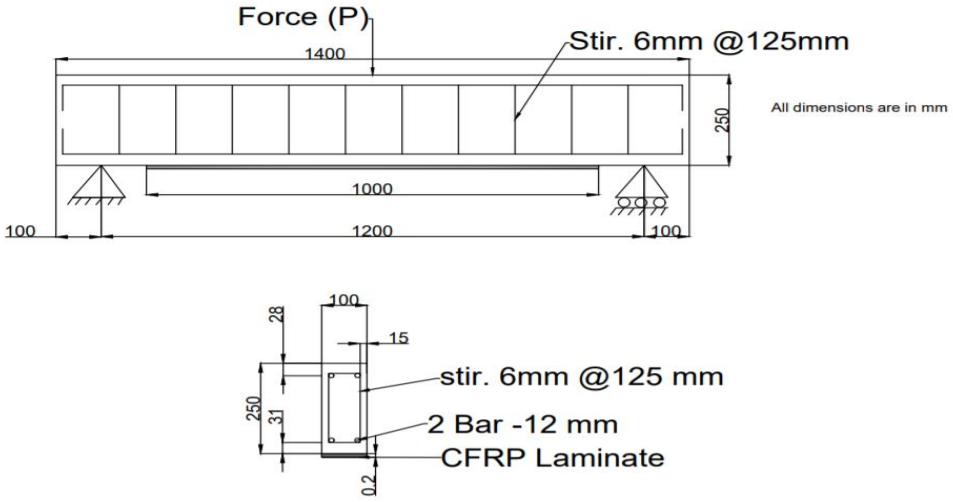

Figure 1 Reinforcement details of CFRP beam

Sensitivity analysis

Strain and temperature sensitivities of FBG arises from the refractive index change and grating period variation. Usually, the strain sensitivity is about 1 nm/μ€ (μ€=micro strain) and temperature sensitivity is about 13 pm/°C for a standard FBG sensor around 1550nm wavelength. Such high sensitivity enables to measure strain and temperature with comparably high resolution and precision.

The RCC beam and CFRP beam is modelled considering temperature varying at 0 -100 °C at 5°C intervals keeping load constant by utilizing FEA software Abaqus for analysis. The materials used for modelling RCC and CFRP beam with temperature are created by adding their material properties shown in Table 2. Thermal expansion of concrete is added. The co efficient of thermal expansion α is taken $12x10^{-6}$/°C. The Concrete beam and steel reinforcement are defined as solid homogeneous section as shown in the Figure 2.

Table 2 Material properties of RCC and CFRP beam with thermal expansion (Chansawat et al., 2009)

Material	Modulus of elasticity (kN/m^2)	Poisson's ratio	Thermal expansion α
Concrete	$3.16x10^7$	0.21	$12x10^{-6}$/°C
CFRP	$2.28x10^6$	0.21	$12x10^{-6}$/°C

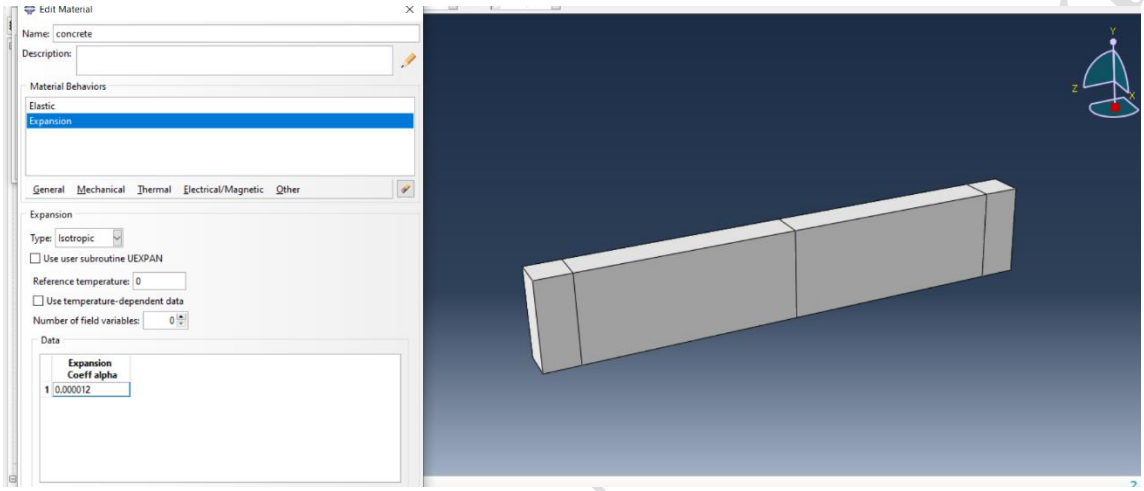

Figure 2 Assigning material property to CFRP beam

Boundary conditions

These are the constraints that are necessary for solving boundary value problems. A boundary value problem is a differential equation to be solved in a domain on whose boundary a set of condition is known. The boundary conditions are known parameters such as load or displacements applied on the model. Boundary conditions are created where-in the 1st condition is applied at the bottom of the beam with a roller support shown in figure-. The 2nd condition is applied vertically and the constant load of 60 kN is applied at the midpoint is shown figure 3. The RCC beam and CFRP beam is subjected to thermal loads varying at 0 -100 °C at 5°C intervals. The Figure 4 showing the beam with initial temperature 0°C and final temperature 60°C.

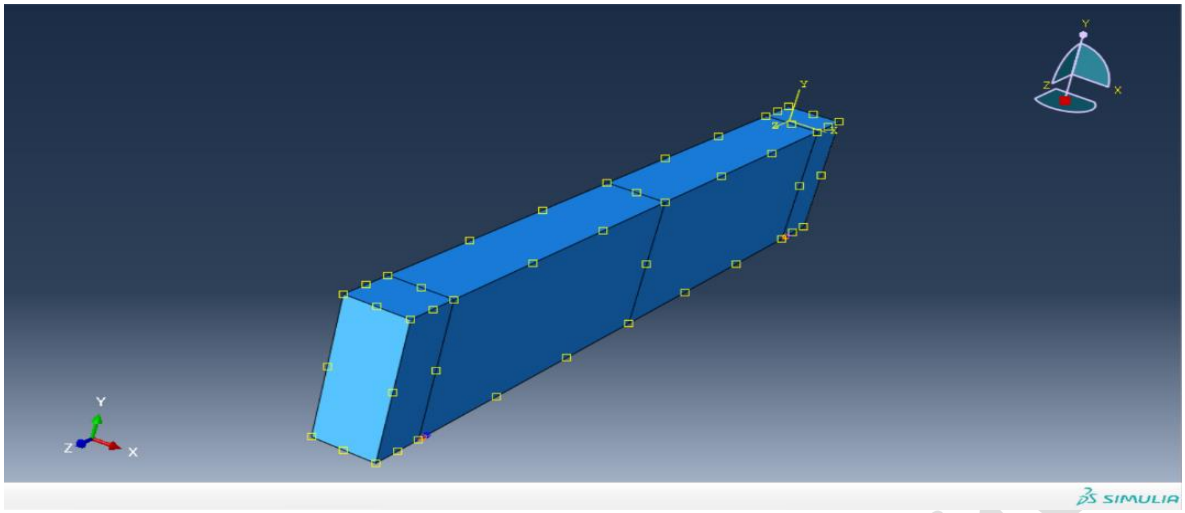

Figure 3 3D Model of beam with boundary conditions

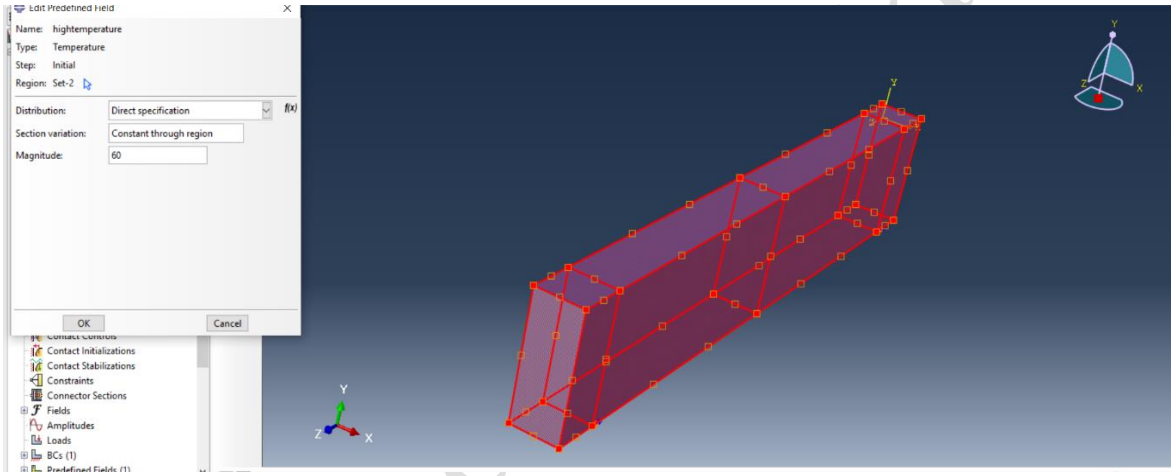

Figure 4 3D Model of beam with applied temperature

Modeling of concrete beam subjected to bending test

The behavior of reinforced concrete structural elements when subjected to various loading conditions is very important to assess the performance of it. Among the various factors influencing the performance of concrete, flexural or bending resistance plays a very important role. Flexural strength of concrete indicates the resistance of concrete to bending failure and is expressed in terms of Modulus of Rupture (MR). This strength can be measured by subjecting a concrete beam to center point or three-point loading. In a centre point test, beam fails near the midpoint whereas in the case of three point loading the beam fails at the weakest portion which falls in the middle third of the beam. In this study, the flexure strength is determined through center point loading as the main aim is to obtain the displacement. A three-dimensional reinforced concrete beam is numerically modelled using Finite Element Analysis (FEA)-based

Abaqus software. The length of the beam modelled is 1400 mm and its cross section is 100 mm x 250 mm as shown in Fig.5.

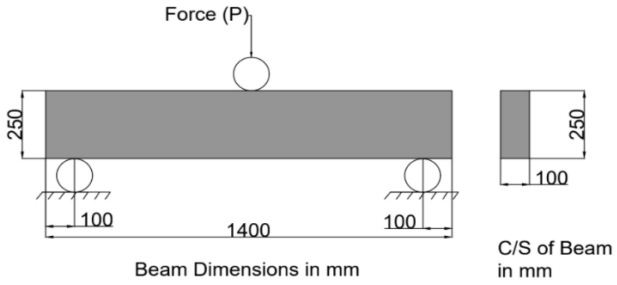

Fig. 5 RCC beam under three-point bending arrangement

The concrete is considered to be of M40 grade. Reinforcement bars of 12mm diameter and stirrups of 4mm diameter is used in modelling this beam. Concrete beam and steel reinforcement are defined as a solid homogeneous section. The beam is loaded gradually to a peak value, at 5-kN intervals until a crack is formed.

Simulation using Abaqus

The different stages of Abaqus simulation include pre-processing, simulation and post-processing. The pre-processing step is also known as modelling. In this step, the model part, material properties, interactions and boundary conditions are created. This input file is created graphically using Abaqus. After pre-processing the model is simulated in Abaqus/ Standard or Abaqus/ Explicit. Once the simulation has been completed, the post-processing step evaluates the displacement, reaction forces and other fundamental variables.

Meshing

The accuracy of any FEA model obtained is directly related to the finite element mesh that is used for the model (Fig. 6 and 7). Decreasing the mesh size always increases the accuracy but also increases computational cost. Meshing generally breaks the model parts into pieces which are termed as elements. Meshing of the model is required to get the accurate results. As discretization of the model is directly related to accuracy, it is important to be careful while meshing the model. In the current study three-dimensional tetrahedral mesh element from the Abaqus library is considered from meshing the geometry. Three-dimensional meshing technique can handle large variations in elements size. It can be applied to almost any three-dimensional region; very complex models can be meshed using this technique(Lima et al., 2021).

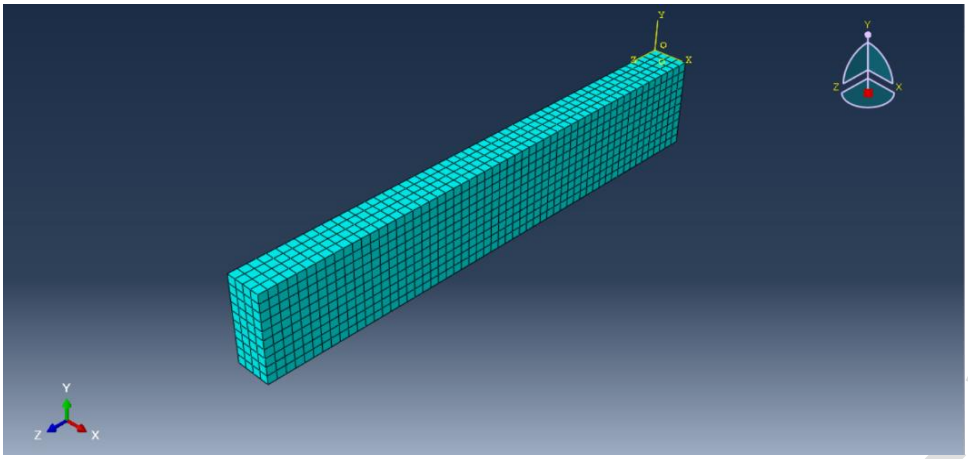

Figure 6 Meshing of concrete beam

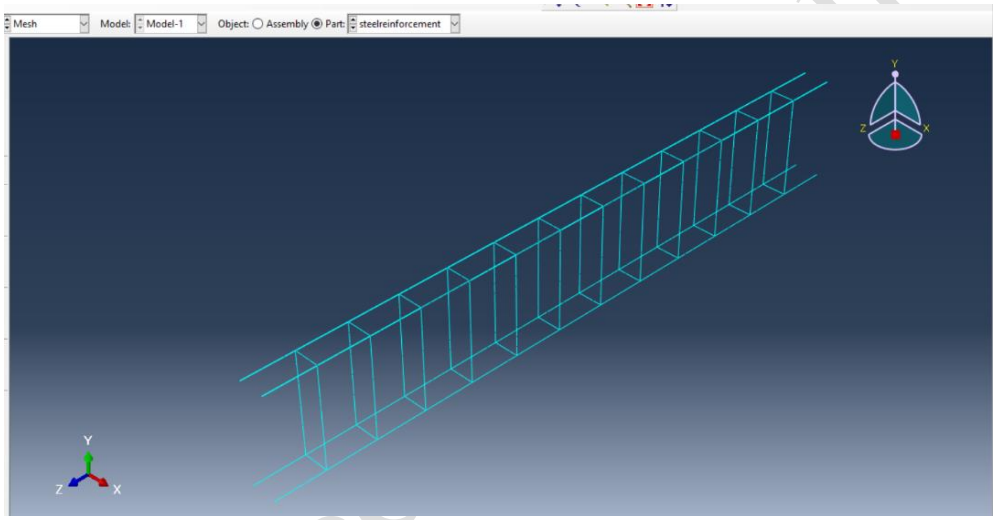

Figure 7 Meshing of steel reinforcement

Results and Discussion

Stresses and displacement of RCC beam

The maximum stress distribution on RCC beam subjected to three-point bending at 60 kN loading is 17.3 MPa is shown in the Figure 8. The displacement is maximum at the midpoint. The displacement increases with increase in loading. The displacement obtained at 60 kN is 0.5334mm shown in Figure 9.

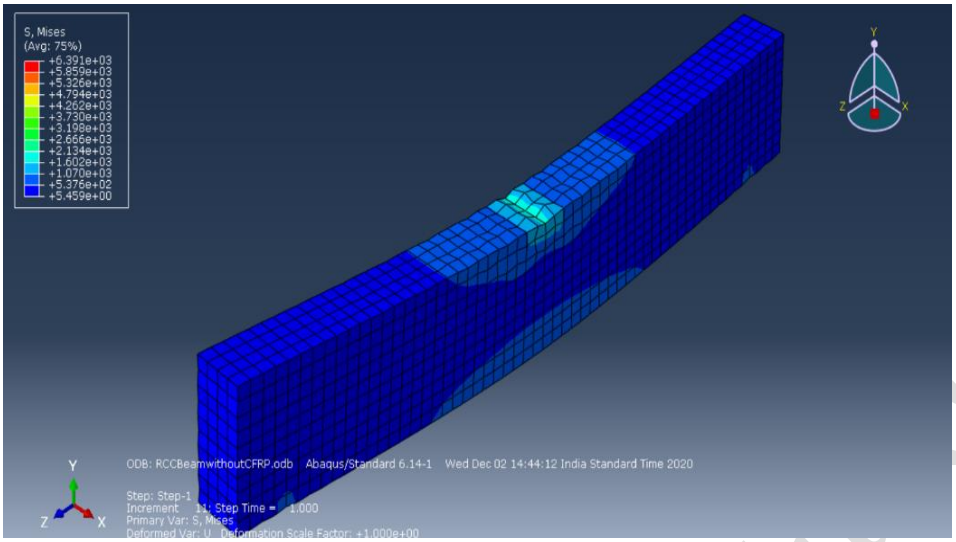

Figure 8 Stress distribution on RCC beam

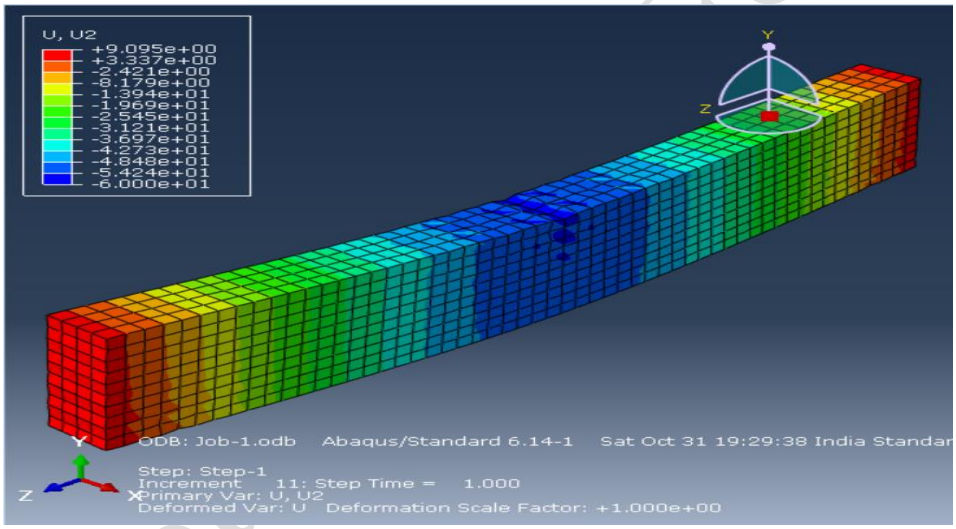

Figure 9 Displacement of RCC beam

Validation of results

The displacement of RCC beam obtained at 60 kN is compared with the results obtained from numerical and analytical. The analysis results obtained from Abaqus is used to plot linear graph of horizontal displacement versus applied load, the obtained graph is in a straight line. This obtained linear graph is compared with the graph from the journal paper, where Figure 10 indicates validation result from numerical analysis and Figure 11 shows the validation result from all the three analysis. The comparison of experimental, numerical and analytical methods has been shown in Table 3.

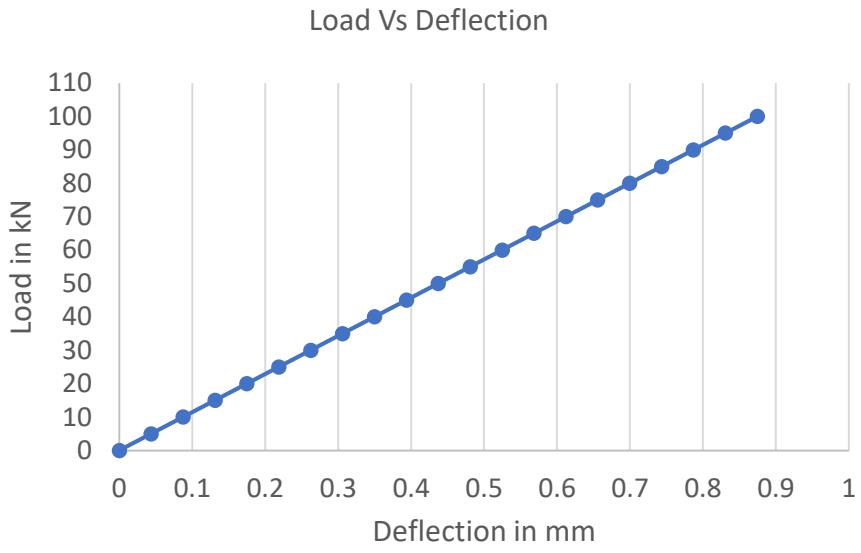

Figure 10 Load vs deflection graph of RCC beam

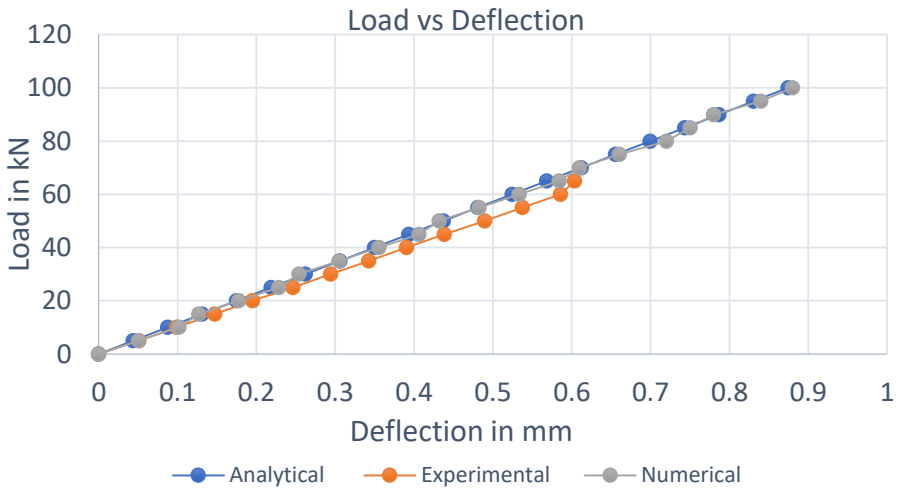

Figure 11 Validation result from numerical analysis

From the above plot of numerical analysis, maximum displacement (x axis) of 0.5334 mm at loading (y axis) = 60 kN. Similarly, from the linear plot from the experimental analysis maximum displacement (x axis) 0.5855 mm at applied load (y axis) = 60 kN.

Table 3 Comparison of Experimental, Numerical and Analytical methods

Analysis type	Applied force (kN)	Maximum displacement in mm

Experimental Kaklauskas et al. (2019)	60	0.5855
Numerical	60	0.5334
Analytical	60	0.5245

It is observed that the result after analysis and the observed by Kaklauskas et al. (2019) are well acceptable with an error of around 8.86%. Therefore, the further analysis for this dissertation can be carried out with the numerically modelled RCC beam for crack detection. An RCC beam is numerically modelled and analyzed using FEM. The table 3 presents a comparison of maximum displacement values obtained from three different analysis approaches experimental, numerical, and analytical under a consistent applied lateral force of 60 kN. The experimental test, following the methodology of Kaklauskas et al. (2019), recorded the highest displacement of 0.5855 mm, reflecting the actual behavior of the specimen under cyclic loading. The numerical model, likely based on finite element simulation, yielded a slightly lower displacement of 0.5334 mm, suggesting a good correlation with the experimental data while maintaining computational efficiency(Gomes et al., 2025). The analytical approach, which relies on simplified equations and assumptions, predicted the lowest displacement of 0.5245 mm. While all three methods show consistent trends, the differences highlight the increased stiffness typically assumed in analytical models and the greater precision of numerical simulations(Mandal and Sidhishwari, 2025). The methods validates the accuracy of the numerical and analytical models in capturing the structural response under the specified loading condition(Kaklauskas et al., 2019).

Stresses and displacement of CFRP concrete beam

The maximum stress distribution on CFRP beam subjected to three-point bending at 60 kN loading is 3.37 MPa is shown in the Figure 12. The displacement is maximum at the midpoint. The displacement increases with increase in loading. The displacement of CFRP beam obtained at 60 kN is 0.0727mm as shown in Figure 13. The graph is plotted for loads applied to strain obtained in Figure 14.

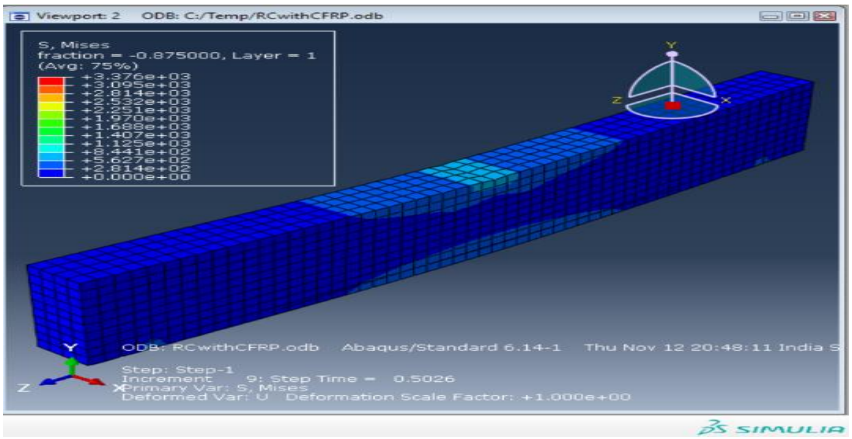

Figure 12 Stress distributions in CFRP beam

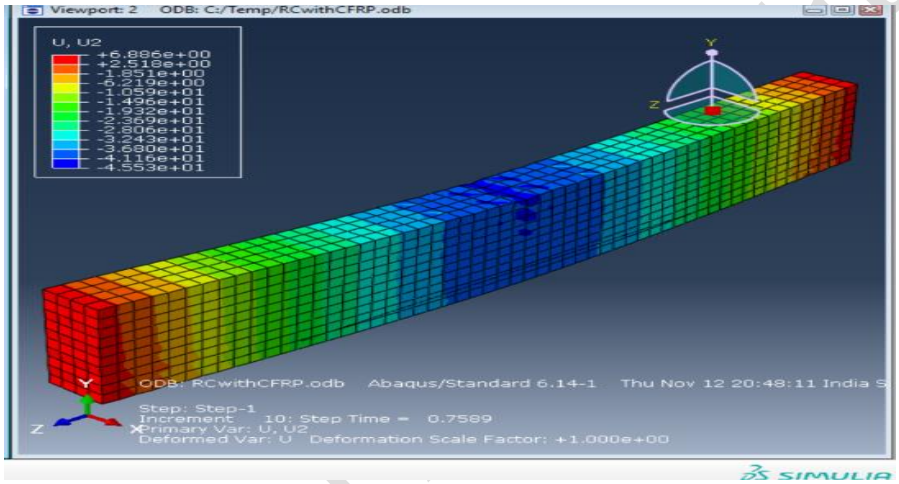

Figure 13 Displacement of the CFRP beam

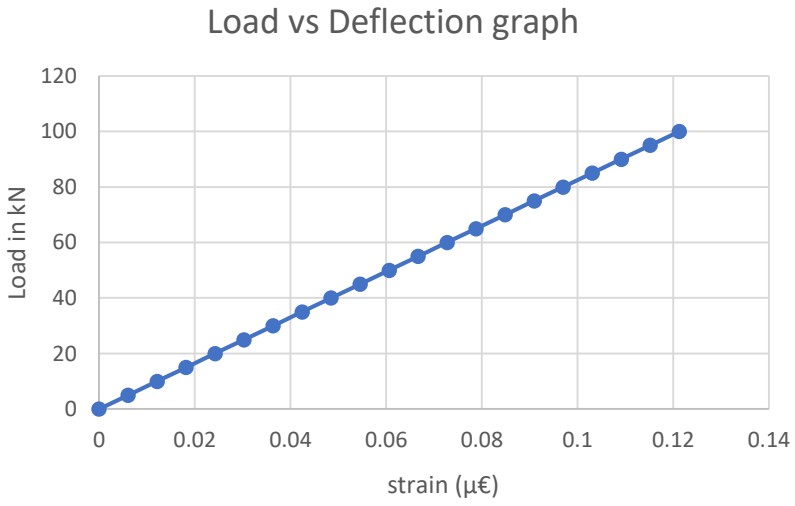

Figure 14 Load vs deflection plot for CFRP beam

Table 4 Comparison of results obtained from RCC and CFRP beam

Type of beam	Applied force in kN	Maximum displacement in mm
RCC beam	60	0.5245
CFRP strengthened concrete beam	60	0.0727

The results in Table 4 show that the deflection of CFRP strengthened beam is 86% lesser to that of RCC beam. This result shows that strengthened beam have more stiffness compared to concrete beam. The table 4 compares the structural response of RCC beam and a CFRP-strengthened concrete beam under the same applied lateral force of 60 kN. The RCC beam exhibited a maximum displacement of 0.5245 mm, indicating its relatively lower stiffness and higher deformation under load. In contrast, the CFRP-strengthened beam showed a significantly reduced displacement of 0.0727 mm an approximate 86% decrease demonstrating a substantial improvement in stiffness and load resistance due to the CFRP confinement(Song et al., 2023). This dramatic reduction in displacement highlights the effectiveness of CFRP strengthening in enhancing structural performance by limiting deformations, increasing rigidity, and potentially delaying the onset of cracking or yielding(Rousan et al., 2024). The results confirm that CFRP wrapping provides considerable confinement and reinforcement, making it a highly effective retrofit technique for improving the structural behavior of concrete beams subjected to lateral or cyclic loading(Soman et al., 2025).

FBG analysis

The shift in Bragg wavelength equation simulated in earlier section is used for the prediction of deflection obtained in RCC and CFRP beam is plotted as wavelength shift vs strain as shown in Figure 15 and Figure 16.

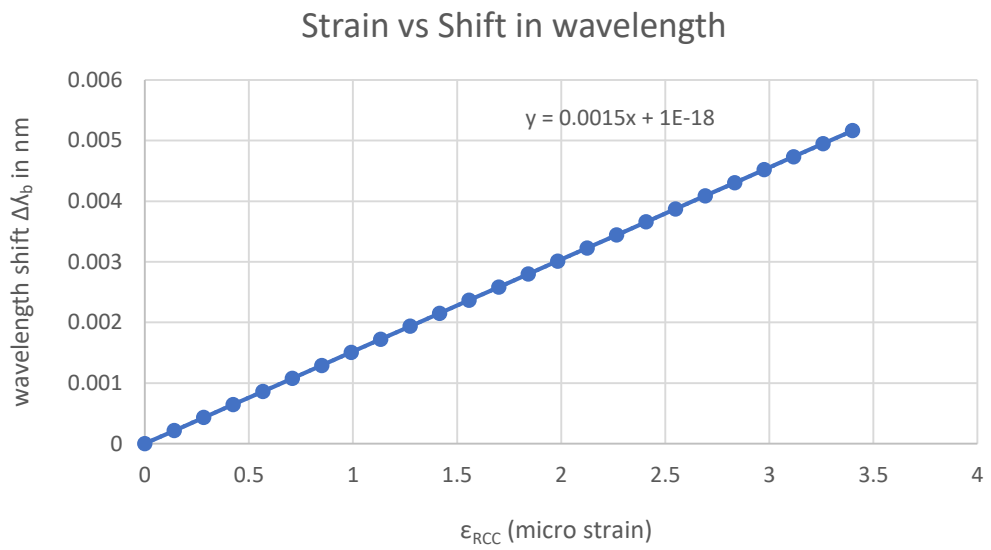

Figure 15 Strain vs wavelength shift in RCC beam

Fig 15 shows linearly increasing shift in wavelength with respect to the strain obtained from numerical analysis of normal RCC beam.

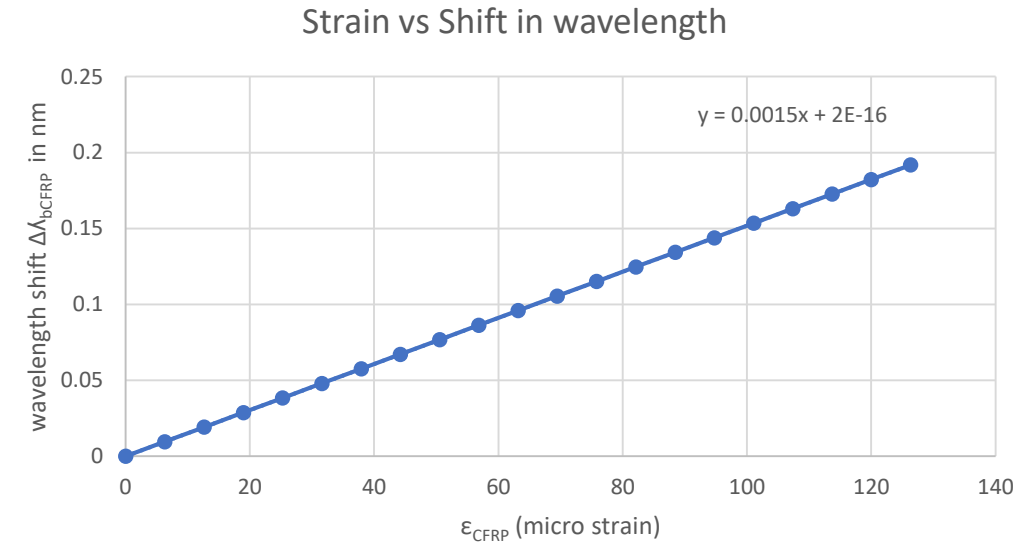

Figure 16 Strain vs wavelength shift in CFRP beam

Fig. 16 shows linearly increasing shift in wavelength with respect to the strain in a CFRP beam. Here, the strain obtained by numerical analysis is relatively more when compared with the latter RCC beam. The results show that, the stress and strain variation of CFRP concrete beam is 86% lesser than the RCC beam. It is clearly seen that strengthened concrete beam has more

stiffness compared to concrete beam. Hence CFRP beam is best material for strengthening existing structures.

Sensitivity results

Stresses and displacement of RCC beam with thermal loads

The RCC and CFRP beam with varying temperature subjected to three-point bending at temperature 60°C has obtained thermal stress of 53.76 MPa and 16.28 MPa is shown in the Figure 17 and 18. The displacement obtained at 60 kN is 1.72mm seen in Figure 19 and 20. Temperature vs Strain graph of RCC and CFRP beam is plotted for temperature varying at 0-100°C as shown in Figure 21 and 22.

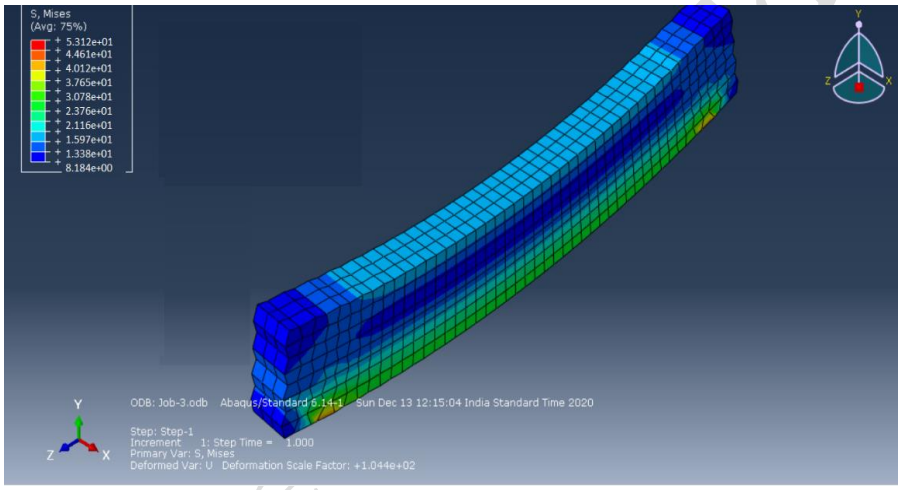

Figure 17 Thermal stress distribution in RCC beam

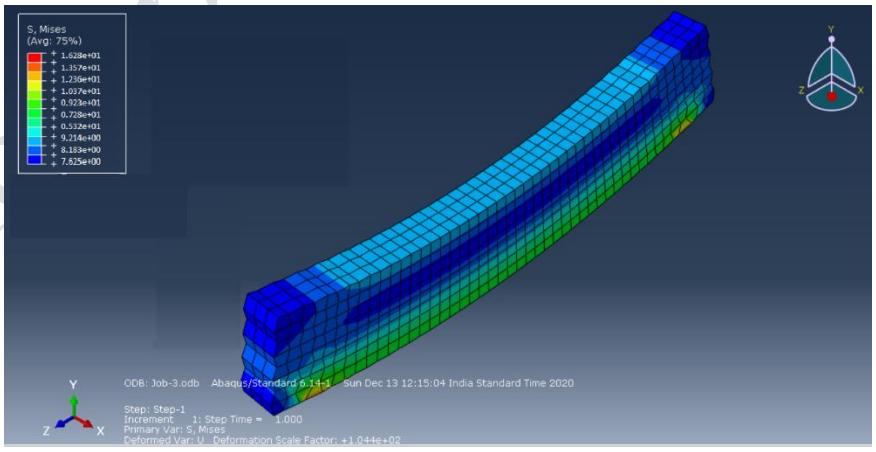

Figure 18 Thermal stress distribution in CFRP beam

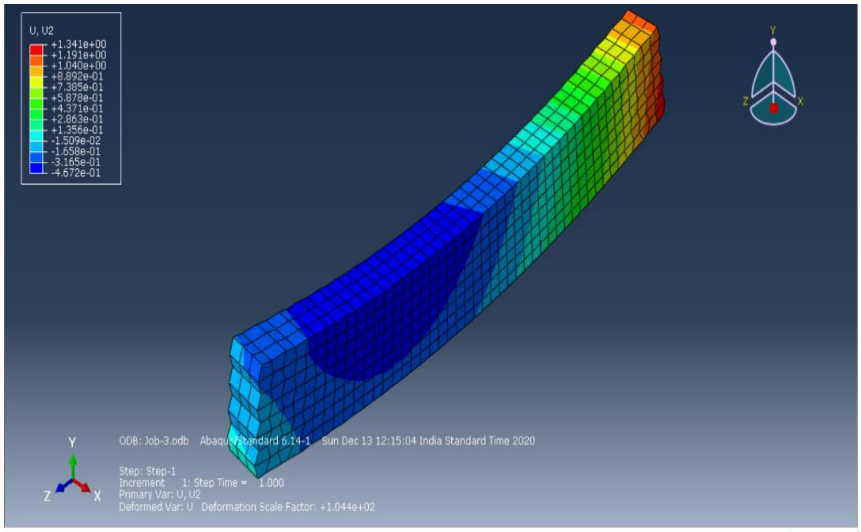

Figure 19 Displacement of RCC beam with thermal loading

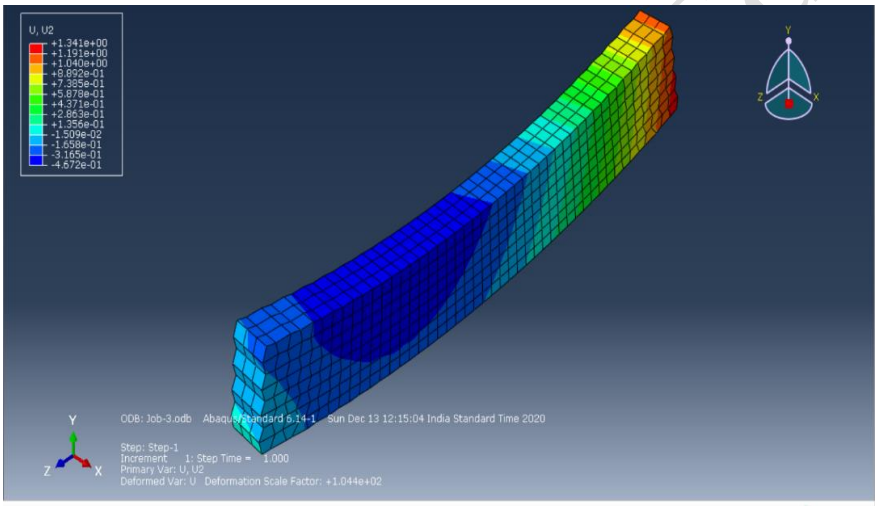

Figure 20 Displacement of CFRP beam with thermal loading

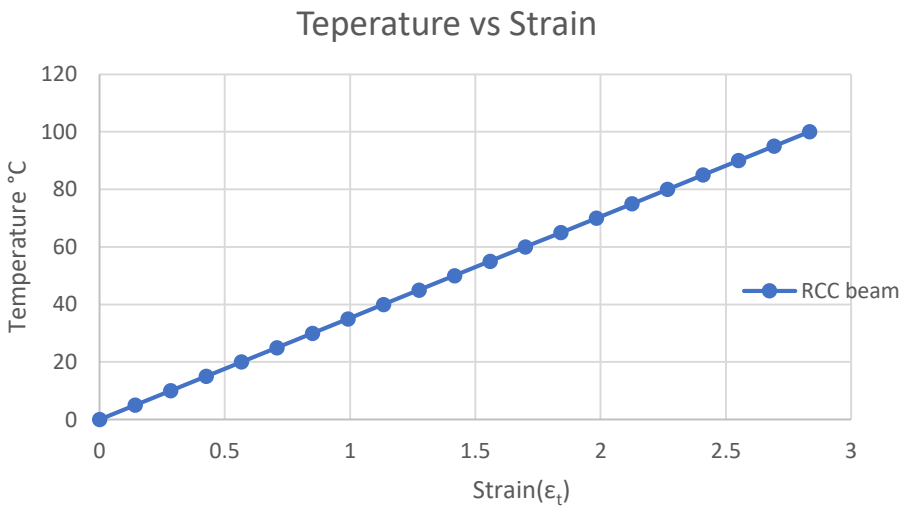

Figure 21 Temperature Vs strain plot of RCC beam

The temperature vs strain graph from Figure 21, it is seen that as temperature is raised in RCC beam the strain is also increasing. The graph obtained is linear in nature.

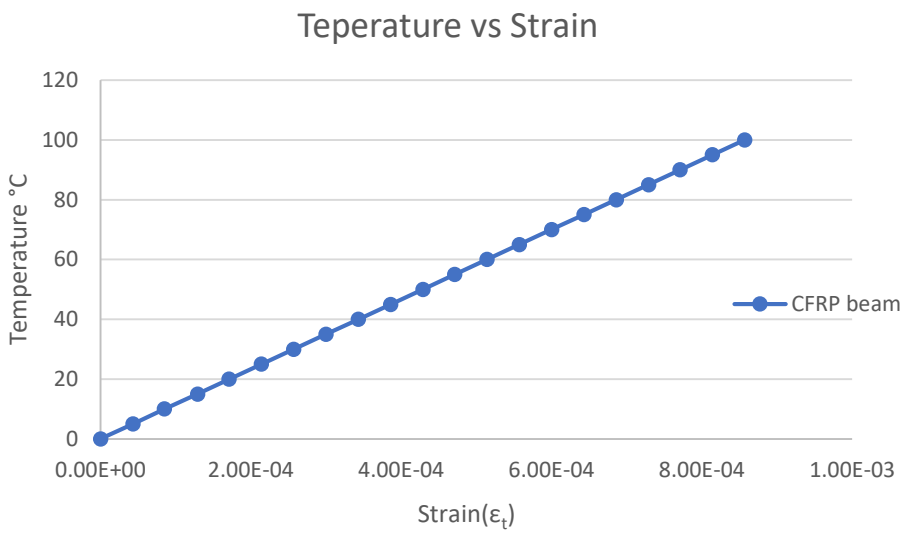

Figure 22 Temperature vs strain plot of CFRP beam

The temperature vs strain graph from Figure 22, it is seen that as temperature is raised in CFRP beam the strain is also increasing. The graph obtained is linear in nature.

Table 5 Comparison of stresses and thermal stresses in beam

Type of beam	Applied load in kN	Temperature °C	Stress in MPa
RCC beam	60	0	17.37
RCC beam subjected to thermal loading	60	100	89.6
CFRP beam	60	0	3.37
CFRP beam subjected to thermal loading	60	100	19.5

The results shown in Table 5 it is seen that RCC beam at 0°C the stress obtained is 17.37 MPa and when the temperature is raised to 60°C in RCC beam the stress are increased by 3 times.

Whereas, the thermal stress obtained in CFRP beam is increased by just 3% when compared to its normal stresses. The results show that CFRP beam is 70% more efficient to thermal loading when compared to RCC beam. At room temperature, the RCC beam experiences a stress of 17.37 MPa, while the CFRP-strengthened beam shows a significantly lower stress of 3.37 MPa, indicating improved load distribution and confinement due to CFRP. However, when exposed to 100 °C, the RCC beam's stress rises sharply to 89.6 MPa over five times higher indicating substantial degradation, likely due to thermal expansion and reduced material strength(Deng et al., 2021; Tan et al., 2021). In contrast, the CFRP-strengthened beam shows only a moderate increase in stress to 19.5 MPa under the same thermal conditions. These results suggest that CFRP wrapping not only improves structural performance under normal conditions but also provides thermal resilience by limiting stress concentrations(Deng et al., 2020). Thus, CFRP strengthening offers a dual benefit of enhanced mechanical and thermal performance, making it a viable solution for structures exposed to elevated temperatures(Kumar et al., 2023). A new subsection has been added comparing our findings with those of Rousan et al. (2024) and Song et al. (2023). Our results align with these studies in terms of increased load capacity and ductility, but our work differs by incorporating a distinct confinement method and pre-damage condition, offering a novel perspective on CFRP performance under cyclic loading. The Mander confinement model aligns with CFRP's role in reducing stress through lateral pressure, but neither Mander nor Kent-Park fully accounts for thermal strains(Xia et al., 2025). Kent-Park's simplified approach, which assumes residual strength, does not predict the drastic stress rise under heating, while Mander's strength enhancement theory partially explains CFRP's benefits. Thus, while CFRP improves performance, a coupled thermo-mechanical model is needed to accurately predict stresses under combined loading(Bai et al., 2025).

FBG analysis for RCC and CFRP beam subjected to temperature

The same mathematical equation simulated for strain parameter of FBG sensor is used for predicting deflection when the temperature is added to RCC beam. The shift in FBG wavelength for varying temperature is shown in Figure 23.

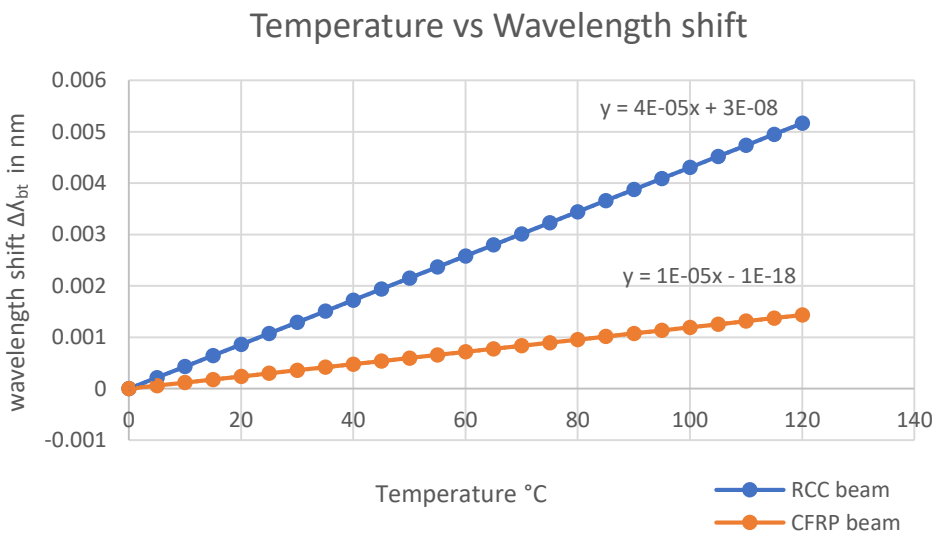

Figure 23 Temperature vs wavelength shift of RCC beam

The Figure 23 shows linearly increasing shift in wavelength with respect to the thermal strains obtained from numerical analysis of RCC and CFRP beam subjected to temperature.

Calculation of sensitivity

The curve fitting yields a straight-line as shown in equation 3 where slope m represents sensitivity of fiber and c is a constant.

$$\Delta\lambda_B = m\Delta\varepsilon + c \quad \text{……..…….. (3)}$$

The simulation of FBG sensors the strains are obtained from numerical analysis of RCC and CFRP beams are shown in Equations 4 and 5 respectively and depicted in Table 7.

$$\Delta\lambda_{B,RCC} = 0.0015xm + 1E\text{-}18 \quad \text{……..…. (4)}$$

$$\Delta\lambda_{B,CFRP} = 0.0015x + 2E\text{-}16 \quad \text{……..……...… (5)}$$

The simulation of FBG sensors the strains are obtained from numerical analysis of RCC and CFRP beams are shown in Equations 6 and 7 respectively while subjecting to thermal loading. The sensitivity of both the beams is depicted in Table 7.

$$\lambda_{B,T} = 4E\text{-}05x + 3E\text{-}08 \quad \text{……..……..……... (6)}$$

$$\lambda_{B,T} = 1E\text{-}05x + 1E\text{-}08 \quad \text{……..…… (7)}$$

Table 6 Comparison of sensitivity

Type of beam	RCC beam	CFRP beam
Sensitivity of FBG fiber for normal strains	1.81 μm/μƐ	1.21 μm/μƐ
Sensitivity of FBG fiber for thermal strains	1.72 nm/°C	1.19 nm/°C

Results tabulated in Table 6 indicate that the FBG fiber is more sensitive when thermal strains are applied. The proposed high sensitivity FBG-based strain sensor can be used for small amplitude micro strain measurement in harsh environment condition. Table 6 compares the sensitivity of Fiber Bragg Grating (FBG) sensors embedded in RCC and CFRP-strengthened beams for both mechanical and thermal strains. In terms of normal strain sensitivity, the FBG in the RCC beam exhibits a higher value of 1.81 μm/μƐ compared to 1.21 μm/μƐ in the CFRP beam, indicating that strain-induced wavelength shifts are more pronounced in conventional concrete. This suggests that the CFRP confinement may limit strain development due to its higher stiffness and better load distribution(Gomes et al., 2025). Similarly, the thermal sensitivity of the FBG fiber is higher in the RCC beam (1.72 nm/°C) than in the CFRP beam (1.19 nm/°C), likely due to the insulating properties of CFRP materials, which reduce thermal transfer to the sensor(Song et al., 2023; Mandal and Sidhishwari, 2025). These results demonstrate that CFRP wrapping not only affects mechanical performance but also influences how strain and temperature are transferred to embedded sensors, which is critical for accurate structural health monitoring(Song et al., 2023; Rousan et al., 2024).

Conclusion

This study is carried out to predict cracks during deflection under various loading and thermal loading conditions for a CFRP concrete beam and a RCC beam using Optical sensors unlike conventional strain gauge. The following are the outcomes of this study:

- The results obtained from numerical analysis for CFRP beam shows acceptable error of 8.86% comparing with the experimental results. The analysis shows that, the stress

and strain variation of CFRP concrete beam is by 86% lesser than the RCC beam and about 3 times increase in values when the RCC beam is subjected to thermal loading.

- Hence CFRP beam is suitable material for strengthening existing structures. A detailed analysis was performed on the data obtained from FBG sensor simulation. FBG sensors are adapted due to its advantage of high sensitivity and high precision to monitor concrete structures.
- The strain sensitivity of sensor is 1.81 μm/με and 1.21 μm/με for RCC and CFRP beam, respectively. The thermal strain sensitivity of sensors is about 1.72 nm/°C and 1.19 nm/°C of RCC and CFRP beam respectively.
- The reported work focuses on using an Optical sensor (Fiber Bragg Grating) for analyzing strain in beams and structures. This interdisciplinary research enables continuous Structural Health Monitoring (SHM) and provides early warning before any calamity occurs.

Limitations and future scope

Fiber Bragg Grating sensor interrogator is expensive and hence cannot be installed in multiple structures even though the sensors are embedded in structures for continuous monitoring. The incorporation of wireless data acquisition system and machine learning algorithm enabling minimal human intervention unlike the conventional strain gauge based sensor.

Funding : None. No funding to declare.

Data availability: Data will be made available on request from the corresponding author.

Declarations

Conflict of interest: None.

References

Alam, M.A. and Al Riyami, K. (2018). "Shear strengthening of reinforced concrete beam using natural fibre reinforced polymer laminates", Construction and Building Materials, v. 162, p. 683–696, https://doi.org/10.1016/j.conbuildmat.2017.12.011.

Alhussein, A.N.D., Qaid, M.R.T.M., Agliullin, T., Valeev, B., Morozov, O. and Sakhabutdinov, A. (2025). "Fiber Bragg Grating Sensors: Design, Applications, and Comparison with Other Sensing Technologies", Sensors, v. 25, no. 7, p.

2289, https://doi.org/10.3390/s25072289.

Anastasopoulos, D., Reynders, E.P.B., François, S., De Roeck, G., Van Lysebetten, G., Van Itterbeeck, P. and Huybrechts, N. (2022). "Vibration-based monitoring of an FRP footbridge with embedded fiber-Bragg gratings: Influence of temperature vs. damage", Composite Structures, v. 287, p. 115295, https://doi.org/10.1016/j.compstruct.2022.115295.

Bai, Y., An, X., Wang, G., Rong, H., Zhang, Y. and Tao, J. (2025). "Seismic performance of short concrete columns reinforced with steel-FRP composite bars and GFRP stirrups", Case Studies in Construction Materials, v. 22, p. e04703, https://doi.org/10.1016/j.cscm.2025.e04703.

Bao, P., Yuan, M., Dong, S., Song, H. and Xue, J. (2013). "Fiber Bragg grating sensor fatigue crack real-time monitoring based on spectrum cross-correlation analysis", Journal of Sound and Vibration, v. 332, no. 1, p. 43–57, https://doi.org/10.1016/j.jsv.2012.07.049.

Benazzo, F., Rigamonti, D., Bettini, P., Sala, G. and Grande, A.M. (2022). "Interlaminar fracture of structural fibre/epoxy composites integrating damage sensing and healing", Composites Part B: Engineering, v. 244, p. 110137, https://doi.org/10.1016/j.compositesb.2022.110137.

Bernasconi, A., Martulli, L.M. and Carboni, M. (2022). "Fatigue crack growth analysis in composite bonded joints by back face distributed strain sensing and comparison with X-ray microtomography", International Journal of Fatigue, v. 154, p. 106526, https://doi.org/10.1016/j.ijfatigue.2021.106526.

Bersan, S., Bergamo, O., Palmieri, L., Schenato, L. and Simonini, P. (2018). "Distributed strain measurements in a CFA pile using high spatial resolution fibre optic sensors", Engineering Structures, v. 160, p. 554–565, https://doi.org/10.1016/j.engstruct.2018.01.046.

Chansawat, K., Potisuk, T., Miller, T.H., Yim, S.C. and Kachlakev, D.I. (2009). "FE Models of GFRP and CFRP Strengthening of Reinforced Concrete Beams", Advances in Civil Engineering, v. 2009, p. 1–13, https://doi.org/10.1155/2009/152196.

Chen, W.-P., Shih, F.-H., Tseng, P.-J., Shao, C.-H. and Chiang, C.-C. (2015). "Application of a Packaged Fiber Bragg Grating Sensor to Outdoor Optical Fiber Cabinets for Environmental Monitoring", IEEE Sensors Journal, v. 15, no. 2, p. 734–

741, https://doi.org/10.1109/JSEN.2014.2353040.

Deng, J., Li, J. and Zhu, M. (2022). "Fatigue behavior of notched steel beams strengthened by a prestressed CFRP plate subjected to wetting/drying cycles", Composites Part B: Engineering, v. 230, p. 109491, https://doi.org/10.1016/j.compositesb.2021.109491.

Deng, L., Liu, Y., Liao, L., Xie, H., Huang, X., Lai, S. and Zhong, M. (2020). "Investigation of Flexural Fatigue Behavior of Concrete Beams Reinforced with Intelligent CFRP-OFBG Plates", Advances in Civil Engineering, v. 2020, no. 1, https://doi.org/10.1155/2020/1062592.

Deng, L., Zhong, M., Liu, Y., Liao, L., Lai, S., Lei, L. and Zhou, Z. (2021). "Study on the Flexural Fatigue Performance of CFRP-OFBG Plate Reinforced Damaged Steel Beams", KSCE Journal of Civil Engineering, v. 25, no. 12, p. 4686–4697, https://doi.org/10.1007/s12205-021-1138-y.

Fernando, C., Bernier, A., Banerjee, S., Kahandawa, G.G. and Eppaarchchi, J. (2017). "An Investigation of the Use of Embedded FBG Sensors to Measure Temperature and Strain Inside a Concrete Beam During the Curing Period and Strain Measurements under Operational Loading", Procedia Engineering, v. 188, p. 393–399, https://doi.org/10.1016/j.proeng.2017.04.500.

Gomes, S.Y., Saidi, M., Lushnikova, A. and Plé, O. (2025). "Fibre Optic-Based Patch Sensor for Crack Monitoring in Concrete Structures", Strain, v. 61, no. 1, https://doi.org/10.1111/str.12489.

Han, S., Xiao, G., Tan, W., Zhou, A., Yu, J. and Ou, J. (2025). "Effect of axial compression ratio on seismic behavior of hybrid FRP-steel reinforced concrete columns", Engineering Structures, v. 335, p. 120325, https://doi.org/10.1016/j.engstruct.2025.120325.

Harle, S.M. (2024). "Durability and long-term performance of fiber reinforced polymer (FRP) composites: A review", Structures, v. 60, p. 105881, https://doi.org/10.1016/j.istruc.2024.105881.

Holmes, C., Godfrey, M., Bull, D.J. and Dulieu-Barton, J. (2020). "Real-time through-thickness and in-plane strain measurement in carbon fibre reinforced polymer composites using planar optical Bragg gratings", Optics and Lasers in Engineering, v. 133, p. 106111, https://doi.org/10.1016/j.optlaseng.2020.106111.

Ikeda, Y., Takeda, S., Hisada, S. and Ogasawara, T. (2024). "Detection of matrix cracks in composite laminates using embedded fiber-optic distributed strain sensing", Sensors and Actuators A: Physical, v. 380, p. 116039, https://doi.org/10.1016/j.sna.2024.116039.

IS 456. (2000). "Concrete, Plain and Reinforced", Bureau of Indian Standards, New Dehli, p. 1–114.

Jovarauskaite, G., Monastyreckis, G., Mishnaevsky, L. and Zeleniakiene, D. (2025). "Self-sensing composites with damage mapping using 3D carbon fibre grid", Composites Part B: Engineering, v. 295, p. 112182, https://doi.org/10.1016/j.compositesb.2025.112182.

K., C., S., M., S., A. and K., S. (2024). "Modelling and Simulation of Fiber Bragg Grating Sensors for Temperature and Pressure Measurements in Environmental Monitoring Station", IEEE North Karnataka Subsection Flagship International Conference (NKCon), p. 1–5, https://doi.org/10.1109/NKCon62728.2024.10775279.

Kaklauskas, G., Sokolov, A., Ramanauskas, R. and Jakubovskis, R. (2019). "Reinforcement Strains in Reinforced Concrete Tensile Members Recorded by Strain Gauges and FBG Sensors: Experimental and Numerical Analysis", Sensors, v. 19, no. 1, p. 200, https://doi.org/10.3390/s19010200.

Kumar, P., Pratap, B., Sharma, S. and Kumar, I. (2023). "Compressive strength prediction of fly ash and blast furnace slag - based geopolymer concrete using convolutional neural network", Asian Journal of Civil Engineering, https://doi.org/10.1007/s42107-023-00861-5.

Lima, R.A.A., Migliavacca, F., Martulli, L.M., Carboni, M. and Bernasconi, A. (2022). "Distributed fibre optic monitoring of mode I fatigue crack propagation in adhesive bonded joints and comparison with digital image correlation", Theoretical and Applied Fracture Mechanics, v. 121, p. 103501, https://doi.org/10.1016/j.tafmec.2022.103501.

Lima, R.A.A., Perrone, R., Carboni, M. and Bernasconi, A. (2021). "Experimental analysis of mode I crack propagation in adhesively bonded joints by optical backscatter reflectometry and comparison with digital image correlation", Theoretical and Applied Fracture Mechanics, v. 116, p. 103117, https://doi.org/10.1016/j.tafmec.2021.103117.

Liu, T., Fu, Y., Li, K., Zhou, A., Qin, R. and Zou, D. (2025). "Experimental investigation and theoretical analysis of long-term performance for optical fiber Bragg grating-fiber

reinforced composite in alkaline concrete environment", Case Studies in Construction Materials, v. 22, p. e04130, https://doi.org/10.1016/j.cscm.2024.e04130.

Liu, Y., Xie, J., Liu, S., Zhao, Y., Zhu, Y. and Qi, G. (2022). "Research on the methodology of development and calibration of flexible encapsulated fiber Bragg grating sensors", Measurement, v. 201, p. 111730, https://doi.org/10.1016/j.measurement.2022.111730.

Liu, H., Yang, H., Qiao, X., Wang, Y., Liu, X., Lee, Y.-S., Lim, K.-S. and Ahmad, H. (2017). "Curvature and Temperature Measurement Based on a Few-Mode PCF Formed M-Z-I and an Embedded FBG", Sensors, v. 17, no. 8, p. 1725, https://doi.org/10.3390/s17081725.

Mandal, H.N. and Sidhishwari, S. (2025). "Apodized chirped fiber Bragg grating for measuring the uniform and non-uniform characteristics of physical parameters", Measurement, v. 240, p. 115606, https://doi.org/10.1016/j.measurement.2024.115606.

Manterola, J., Aguirre, M., Zurbitu, J., Renart, J., Turon, A. and Urresti, I. (2020). "Using acoustic emissions (AE) to monitor mode I crack growth in bonded joints", Engineering Fracture Mechanics, v. 224, p. 106778, https://doi.org/10.1016/j.engfracmech.2019.106778.

Mao, J., Xu, F., Gao, Q., Liu, S., Jin, W. and Xu, Y. (2016). "A Monitoring Method Based on FBG for Concrete Corrosion Cracking", Sensors, v. 16, no. 7, p. 1093, https://doi.org/10.3390/s16071093.

Rousan, R.Z., Abdalla, K.M. and Alnemrawi, B.R. (2024). "The Behavior of Heat-Damaged RC Beams Reinforced Internally with CFRP Strips", 4th International Conference "Coordinating Engineering for Sustainability and Resilience" & Midterm Conference of CircularB “Implementation of Circular Economy in the Built Environment”, p. 165–174, https://doi.org/10.1007/978-3-031-57800-7_15.

Sakiyama, F.I.H., Lehmann, F. and Garrecht, H. (2021). "Structural health monitoring of concrete structures using fibre-optic-based sensors: a review", Magazine of Concrete Research, v. 73, no. 4, p. 174–194, https://doi.org/10.1680/jmacr.19.00185.

Saleem, M.U., Qureshi, H.J., Amin, M.N., Khan, K. and Khurshid, H. (2019). "Cracking Behavior of RC Beams Strengthened with Different Amounts and Layouts of CFRP", Applied Sciences, v. 9, no. 5, p. 1017, https://doi.org/10.3390/app9051017.

Sellami, F., Memmolo, V. and Hornung, M. (2025). "Guided Wave Propagation in a Realistic CFRP Fuselage Panel: Proof of Concept for Early-Stage Damage Detection", Sensors, v. 25, no. 4, p. 1104, https://doi.org/10.3390/s25041104.

Sevillano, E., Sun, R., Perera, R., Arteaga, A., De Diego, A. and Cisneros, D. (2016). "Comparison of PZT and FBG sensing technologies for debonding detection on reinforced concrete beams strengthened with external CFRP strips subjected to bending loads", Materiales de Construcción, v. 66, no. 322, p. e088, https://doi.org/10.3989/mc.2016.05415.

Shishkin, V.V., Terentyev, V.S., Kharenko, D.S., Dostovalov, A.V., Wolf, A.A., Simonov, V.A., Fedotov, M.Y., Shienok, A.M., Shelemba, I.S. and Babin, S.A. (2016). "Experimental Method of Temperature and Strain Discrimination in Polymer Composite Material by Embedded Fiber-Optic Sensors Based on Femtosecond-Inscribed FBGs", Journal of Sensors, v. 2016, p. 1–6, https://doi.org/10.1155/2016/3230968.

Soman, R., Moaf, F.O., Fiborek, P., Kurpińska, M., Sarbaz, S., Karpiński, M. and Wandowski, T. (2025). "Investigating the effect of orientation of polarization maintaining fiber Bragg grating sensor on its sensitivity to fundamental symmetric and antisymmetric guided wave modes", Measurement, v. 252, p. 117307, https://doi.org/10.1016/j.measurement.2025.117307.

Song, S., Tian, Z., Zhao, Z., Li, X., Zhao, J. and Xu, B. (2023). "Experimental Study on Seismic Performance of CFRP-Strengthened Recycled Concrete Columns with Different Levels of Seismic Damage", Buildings, v. 13, no. 6, p. 1470, https://doi.org/10.3390/buildings13061470.

Sourisseau, Q., Lepretre, E., Chataigner, S., Chapeleau, X., Mouton, L. and Paboeuf, S. (2022). "Use of high spatial resolution distributed optical fiber to monitor the crack propagation of an adhesively bonded joint during ENF and DCB tests", International Journal of Adhesion and Adhesives, v. 115, p. 103124, https://doi.org/10.1016/j.ijadhadh.2022.103124.

Srivastava, N.K., Parihar, R. and Raghuwanshi, S.K. (2020). "Efficient Photonic Beamforming System Incorporating a Unique Featured Tunable Chirped Fiber Bragg Grating for Application Extended to the Ku-Band", IEEE Transactions on Microwave Theory and Techniques, v. 68, no. 5, p. 1851–1857, https://doi.org/10.1109/TMTT.2019.2961889.

Tan, X., Abu-Obeidah, A., Bao, Y., Nassif, H. and Nasreddine, W. (2021). "Measurement and visualization of strains and cracks in CFRP post-tensioned fiber reinforced concrete beams using distributed fiber optic sensors", Automation in Construction, v. 124, p. 103604, https://doi.org/10.1016/j.autcon.2021.103604.

Tiwari, P., Singh, V. and Malaviya, M.M. (2025). "Assessment of Polypropylene Fiber for Effect on Fresh and Physical Performance with Durability of Self-Compacted Recycled Aggregate Concrete", Civil Engineering Infrastructures Journal, v. 58, no. 1, p. 15–34, https://doi.org/10.22059/ceij.2024.362561.1943.

Wang, L., Zhu, D., Gu, J., Huang, L., Yi, J. and Song, Z. (2025). "Analysis and prediction of the short-term flexural stiffness of a steel-Fiber Reinforced Polymer composite bar-reinforced concrete beam", Structural Concrete, v. 26, no. 2, p. 1190–1205, https://doi.org/10.1002/suco.202300922.

Xia, Y., Yu, J. and Jiang, C. (2025). "Cyclic behavior of precast beam-to-column connections with locally reactive powder concrete: An experimental and numerical investigation", Structural Concrete, https://doi.org/10.1002/suco.202401362.

Ye, Y., Hu, S., Fan, X. and Lu, J. (2022). "Effect of adhesive failure on measurement of concrete cracks using fiber Bragg grating sensors", Optical Fiber Technology, v. 71, p. 102934, https://doi.org/10.1016/j.yofte.2022.102934.

Ye, X.W., Su, Y.H. and Han, J.P. (2014). "Structural Health Monitoring of Civil Infrastructure Using Optical Fiber Sensing Technology: A Comprehensive Review", The Scientific World Journal, v. 2014, p. 1–11, https://doi.org/10.1155/2014/652329.

Zhang, X., Liu, L., Zheng, Z., Quan, Y., Chen, Z., Cao, J., Zhang, T., Xie, X., Liu, X. and Xiang, P. (2025). "Bending strain progression and damage of asphalt beams based on distributed fibre optic sensors", International Journal of Pavement Engineering, v. 26, no. 1, https://doi.org/10.1080/10298436.2025.2479645.

Zhang, X., Xie, X., Wang, L., Luo, G., Cui, H., Wu, H., Liu, X., Yang, D., Wang, H. and Xiang, P. (2024). "Experimental Study on CRTS III Ballastless Track Based on Quasi-distributed Fiber Bragg Grating Monitoring", Iranian Journal of Science and Technology, Transactions of Civil Engineering, v. 48, no. 4, p. 2413–2427, https://doi.org/10.1007/s40996-023-01319-z.